
2016 8 2 8 30

,

8 1
8 3 8 30
9 1

University of Nottingham

Prof. Atanas. Popov

Fig. 1

(Flexible Piezoelectric Device : FPED)

CO2

CO2

FPED

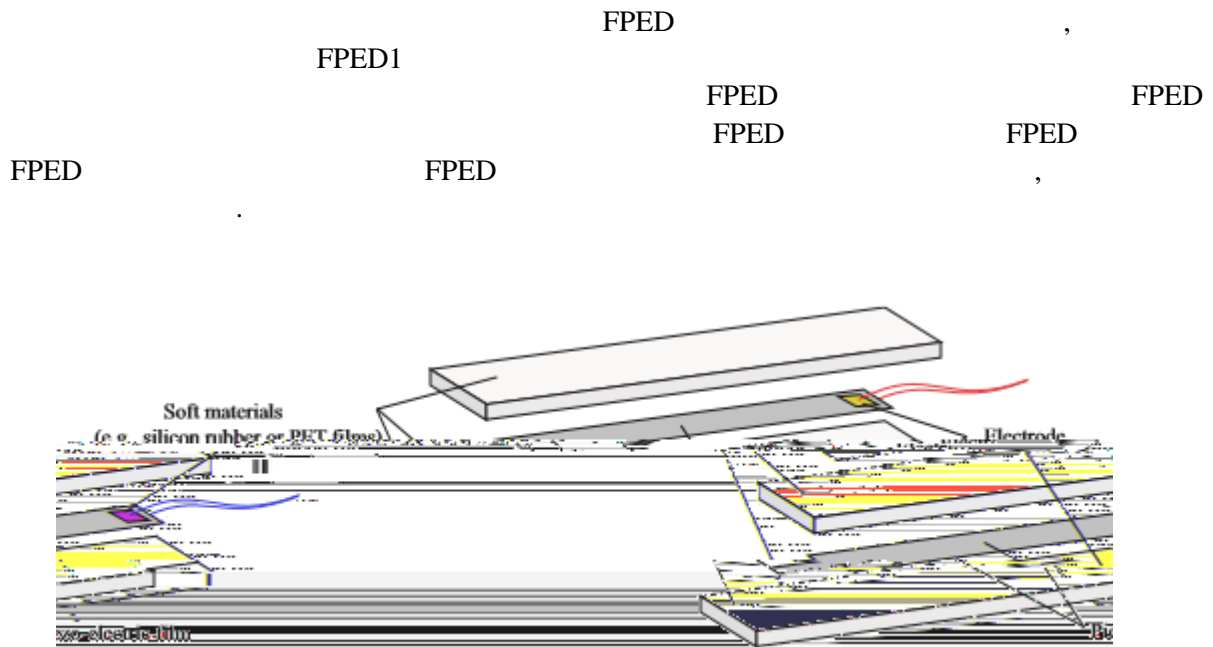


Fig. 1 Basic structure of the FPED

Patel

The diagram illustrates the Transfer Matrix Method (TMM) for a two-dimensional system. It features a central rectangular grid of nodes. The top row contains labels: 'Method' on the left, followed by three blue italicized 'i' symbols, and 'Transfer Matrix' on the right. The bottom row contains labels: 'V' on the left, followed by a blue italicized '2', 'W' in the middle, a blue italicized '4' on the right, 'W' at the bottom left, 'M' at the bottom center, and 'Q' at the bottom right. The grid consists of small squares, with some nodes highlighted in red or yellow.

$$\begin{pmatrix} W(x^{3R}) \\ \theta(x^{3R}) \\ M(x^{3R}) \\ Q(x^{3R}) \end{pmatrix} = (U^3)(I^{32})(U^2)(I^{21})(U^1) \begin{pmatrix} W(x^{1L}) \\ \theta(x^{1L}) \\ M(x^{1L}) \\ Q(x^{1L}) \end{pmatrix} \quad (1)$$

$$\begin{aligned} & \dot{\eta}(t) + 2\gamma\omega\eta(t) + \omega^2\eta(t) \\ &= \dot{\eta}_{base}(t) \int_0^L \mu(x)W(x)dx - \varepsilon V(t)[W(x_1 + x_2) - W(x_1)] \end{aligned} \quad (2)$$

$$C_p \frac{\partial V(t)}{\partial t} + \frac{V(t)}{R_{load}} = -E_p d_{yx} t_{pc} b_p \left[\frac{\partial W(x)}{\partial x} \right]_{x_1+x_2}^{x_1} \eta(t) \quad (3)$$

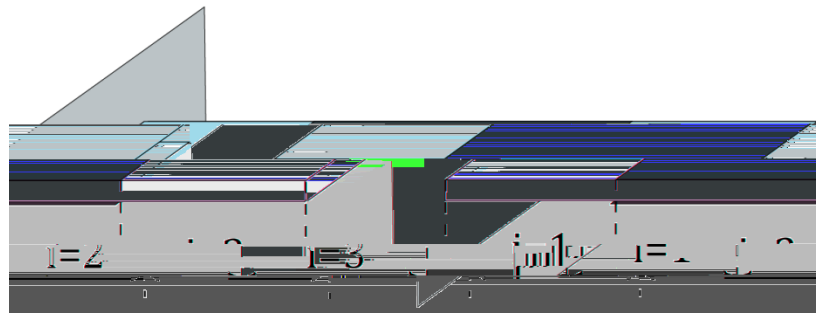


Fig.2 Transfer Matrix Method model of FPED

Fig.3
FPED

FPED

Fig.4

K (N/m)

$$W_1(x^{3RK}) = W_1(x^{3R}) \quad (4)$$

$$Q_1(x^{3RK}) = Q_1(x^{3R}) \quad (5)$$

$$M_1(x^{3RK}) = M_1(x^{3R}) \quad (6)$$

$$Q_1(x^{3RK}) = Q_1(x^{3R}) + K(W_2(x^{3R}) - W_1(x^{3R})) \quad (7)$$

$$W_2(x^{3RK}) = W_2(x^{3R}) \quad (8)$$

$$Q_2(x^{3RK}) = Q_2(x^{3R}) \quad (9)$$

$$M_2(x^{3RK}) = M_2(x^{3R}) \quad (10)$$

$$Q_2(x^{3RK}) = Q_2(x^{3R}) + K(W_1(x^{3R}) - W_2(x^{3R})) \quad (11)$$

(4)~(11)

$$\begin{pmatrix} W_1(x^{3RK}) \\ \theta_1(x^{3RK}) \\ M_1(x^{3RK}) \\ Q_1(x^{3RK}) \\ W_2(x^{3RK}) \\ \theta_2(x^{3RK}) \\ M_2(x^{3RK}) \\ Q_2(x^{3RK}) \end{pmatrix} = \begin{pmatrix} 1 & 0 & 0 & 0 & 0 & 0 & 0 & 0 \\ 0 & 1 & 0 & 0 & 0 & 0 & 0 & 0 \\ 0 & 0 & 1 & 0 & 0 & 0 & 0 & 0 \\ -K & 0 & 0 & 1 & K & 0 & 0 & 0 \\ 0 & 0 & 0 & 0 & 1 & 0 & 0 & 0 \\ 0 & 0 & 0 & 0 & 0 & 1 & 0 & 0 \\ 0 & 0 & 0 & 0 & 0 & 0 & 1 & 0 \\ K & 0 & 0 & 0 & -K & 0 & 0 & 1 \end{pmatrix} \begin{pmatrix} W_1(x^{3R}) \\ \theta_1(x^{3R}) \\ M_1(x^{3R}) \\ Q_1(x^{3R}) \\ W_2(x^{3R}) \\ \theta_2(x^{3R}) \\ M_2(x^{3R}) \\ Q_2(x^{3R}) \end{pmatrix} \quad (12)$$

(12)

FPED 3

W

(2) (3)

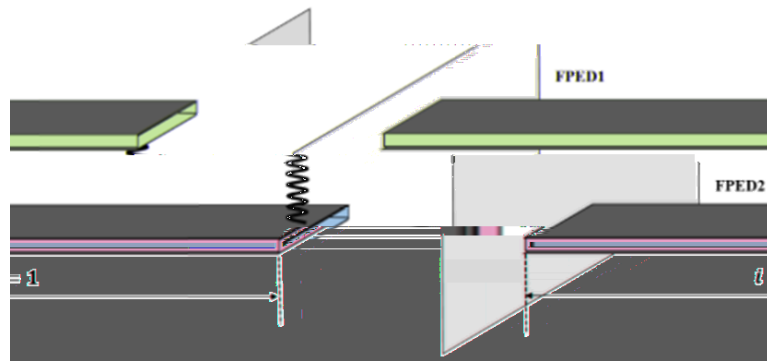


Fig. 3 FPED connected by spring

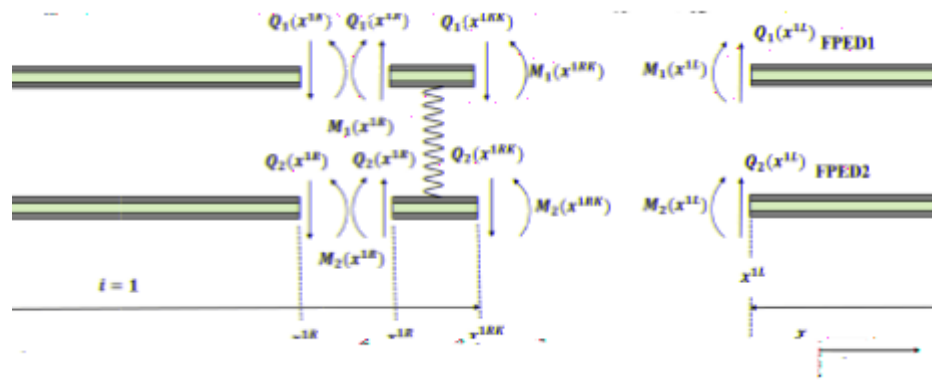


Fig. 4 shear force diagram and bending moment diagram of FPED

Fig.5, Fig.6

FPED

90 (N/m)

490 (N/m)

3

PET

FPED

10m/s^2

10m/s^2

Fig.7

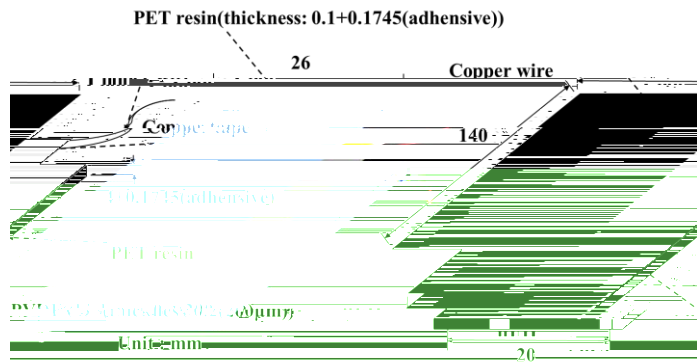


Fig.5 FPED1

—■— Theoretical result Series connection, no spring
—○— Experimental result Series connection, no spring
—▲— Theoretical result Series connection, spring 90 (N/m)
—▼— Experimental result Series connection.spring 90 (N/m)
—◆— Theoretical result Series connection.spring 490 (N/m)
—◆— Experimental result Series connection.spring 490 (N/m)

Fig.6 FPED2

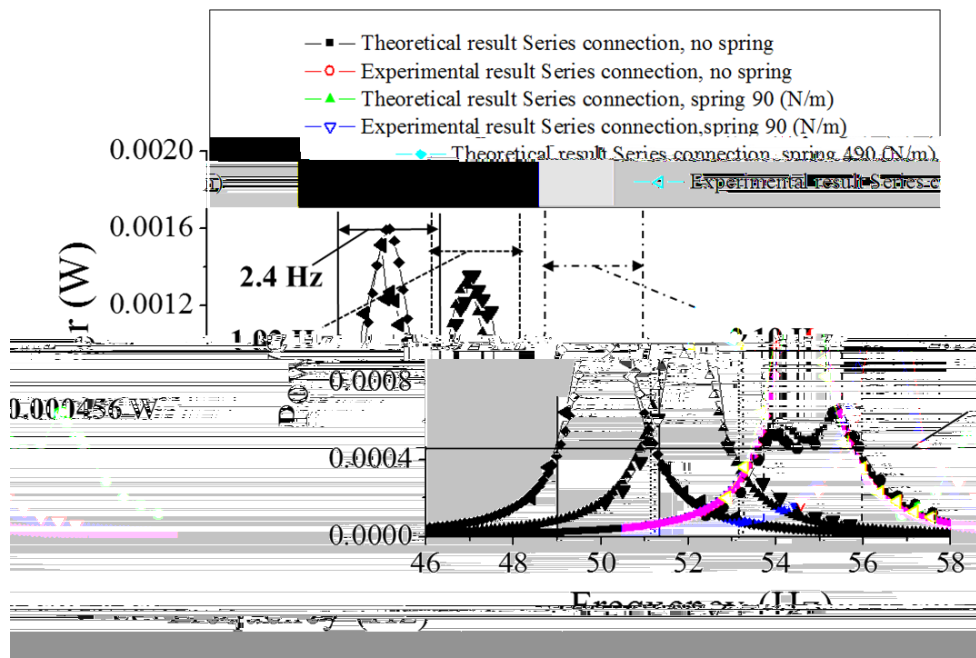


Fig.7 Theoretical result and Experimental result of FPED

FPED FPED FPED
FPED FPED FPED